Temperature-Dependent Kinetic Isotope Effects in the Gas-Phase Reaction: OH + HBr

Veronica I. Jaramillo and Mark A. Smith*

Department of Chemistry, University of Arizona, Tucson, Arizona 85721

Received: November 29, 2000; In Final Form: March 8, 2001

The temperature dependence of the hydrogen transfer rate coefficients for the reactions: OH + HBr (Reaction 1), OD + HBr (Reaction 2), OH + DBr (Reaction 3), and OD + DBr (Reaction 4) have been investigated at temperatures between 120 and 224 K using a pulsed uniform supersonic flow monitoring hydroxyl reactive loss. The lack of observed isotopic scrambling indicates the reaction occurs by H/D atom transfer from HBr/DBr at all temperatures. The rate coefficients demonstrate little temperature dependence above 200 K, but strong inverse temperature behavior below 200 K. The current work provides unequivocal experimental evidence of temperature dependent and inverse primary and secondary kinetic isotope effects ($k_H/k_D < 1$) at low temperatures. The observed kinetic isotope ratios, k_H/k_D, at 120 K are for primary substitution on HBr; $k_1/k_3 = 1.00$ (± 0.17) and $k_2/k_4 = 0.46$ (± 0.08), while for secondary substitution on OH; $k_1/k_2 = 0.94$ (± 0.20) and $k_3/k_4 = 0.43$ (± 0.05). At the lowest temperature employed (120 K), deuterated reactants react as fast or faster than their natural hydrogen isotopomer and there is no significant difference between the primary and secondary kinetic isotope effect. The results are discussed within the framework of recent theoretical models.

Introduction

Isotope distributions in naturally occurring environments provide direct insight into both physical and chemical dynamics. In particular, minor isotopes can play key roles in radiative heat transfer in the interstellar media.[1] Pooling of heavy isotopes into molecular components can occur due to zero point energy differences which can greatly exceed kT in low-temperature media.[2,3] In the case of stratospheric ozone, the debate continues on the origins of the observed terrestrial non-equilibrium isotope distributions.[4] Studies of isotope-specific rate coefficients and kinetic isotope effects can help elucidate origins of particular deviations from natural abundance as well as provide detailed insight into isotope-dependent reaction mechanisms.

The reaction

$$OH + HBr \rightarrow H_2O + Br \quad (1)$$

besides being significant in determining the active bromine fraction in the middle to lower terrestrial stratosphere,[5] has become a well studied bimolecular radical−molecule reaction demonstrating significant non-Arrhenius rate behavior.[6−15] The rate coefficient of Reaction 1 has attracted much attention due to the fact that it displays very weak temperature dependence at higher temperatures, but strong inverse temperature dependence at low temperatures.[13,14,16] Bedjanian et al. have recently investigated the H/D isotope dependence of the reaction between isotopomers of OH and HBr, thus all Reactions 1−4, at temperatures above 230 K.[15]

$$OD + HBr \rightarrow HOD + Br \quad (2)$$

$$OH + DBr \rightarrow HOD + Br \quad (3)$$

$$OD + DBr \rightarrow D_2O + Br \quad (4)$$

The kinetic isotope effect, KIE, is defined for the purpose of this work as the ratio of the rate coefficient observed for a particular reactant pair to the rate coefficient observed when one atom in the reactant pair has been isotopically substituted (for purposes of this paper, replacing H with the heavier D isotope). In this regard, it is also convenient to categorize primary and secondary KIEs. A primary KIE corresponds to one where the atom substituted is involved in a bond being formed or broken along the reaction coordinate. The secondary KIE then involves isotopic substitution associated with bonds not formed or broken during the reaction. The ratios, k_1/k_3 and k_2/k_4 thus correspond to primary kinetic isotope effects, while k_1/k_2 and k_3/k_4 correspond to secondary KIEs. In the study of Bedjanian et al., both of these primary KIEs are found near 1.8, and both secondary KIEs are measured to be near unity. Such observations of normal kinetic isotope ratios are consistent with transition state theory predictions for reactions occurring on potential surfaces with negligible or positive activation barriers. These observations may not be that surprising in the sense that they occur over a temperature window for which Reaction 1 displays no significant temperature dependence.

In view of the strong inverse temperature dependence of Reaction 1 seen below 200 K,[13,14,16] we have investigated the low-temperature rate coefficients of Reactions 1−4. These results show that both the primary and secondary kinetic isotope effects are sensitive functions of temperature below 200 K. More importantly, interesting inverse kinetic isotope ratios ($k_H/k_D <$

* Author to whom correspondence should be addressed at University of Arizona, Department of Chemistry, 1306E, University Drive, Tucson, AZ 85721. Tel: (520) 621-2115. Fax: (520) 621−8407. E-mail: msmith@u.arizona.edu.

10.1021/jp004328q CCC: $20.00
Published on Web 05/19/2001

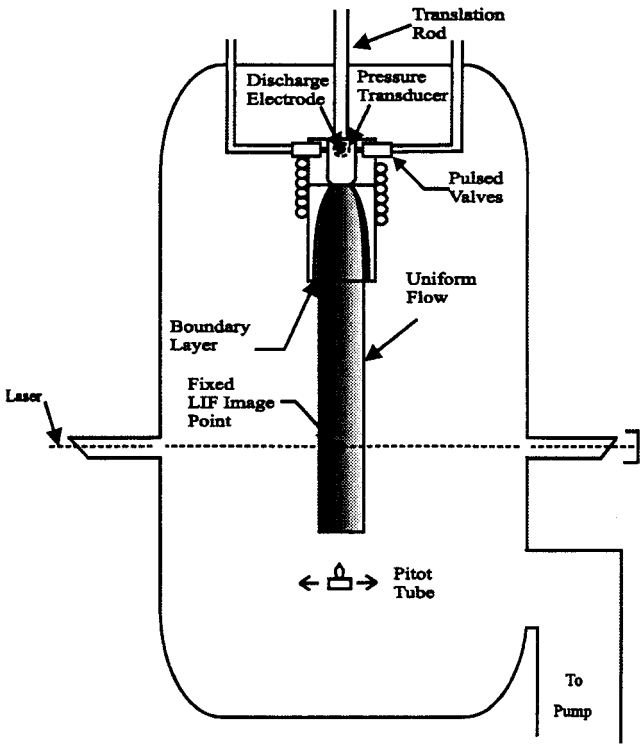

Figure 1. Diagram of the pulsed uniform supersonic flow reactor used in this study.

1) for both primary and secondary substitutions of a bimolecular gas reaction are observed. These results are discussed in the context of recent theoretical models.

Experimental Section

The details of our approach to low-temperature OH radical rate coefficient measurements have been described elsewhere, so only a brief review will be provided here.[14,16,17] The rate coefficients of Reactions 1−4 were determined by laser-induced fluorescence (LIF) monitoring of OH/(OD) concentration under pseudo first-order conditions in a gas flow comprised of HBr/(DBr) seeded in low concentration into the buffer gas, N_2. The first-order rate is obtained from the time-dependent decay of the OH/(OD) LIF signal as a function of flow distance by means common to many flow kinetic methods. Particular to these studies, however, is the way by which the low temperatures are obtained and the nature of the gas flow. The pulsed uniform supersonic flow reactor, shown in Figure 1, employs supersonic expansion of the reaction mixtures within a Laval nozzle to produce a low-temperature uniform density environment, analogous to conventional flow reactors, except with supersonic hydrodynamic velocity and without communication with physical walls. The density conditions of the expansion ensure that the axisymmetric gas flow exiting the nozzle remains in complete local thermodynamic equilibrium at a temperature determined by the controlled nozzle feed conditions of T_0, P_0, and γ, (the latter being the ratio of constant pressure and temperature heat capacities of the expansion mixture), as well as the design contour of the particular nozzle. Using a single buffer/nozzle combination, a particular post-nozzle flow density and temperature may be produced for kinetic studies. In particular for these studies, the reservoir pressure was varied from 6 to 51 Torr, and Mach number from 1.2 to 2.7 (using different nozzle bodies), while the reservoir temperature was held constant at 300 K using a closed cycle liquid temperature controller. These conditions allowed for uniform flows with densities ranging from 3×10^{16} to 2×10^{17} cm^{-3} and flow temperatures from 224 to 120 K. Unfortunately, in these studies we were unable to perform measurements at stagnation temperatures below 300 K and thus with the nozzles available to us, we were limited to a lowest temperature of 120 K for N_2 buffered flows.

The background pressure in this chamber is matched to the internal flow-pressure such that the supersonic flow, once leaving the nozzle body, proceeds without further radial expansion down the reactor vessel. In this way, the reaction flow environment is surrounded by a subsonic gaseous layer (a boundary shock) and does not experience solid walls. This latter point corresponds to one significant difference between these supersonic techniques and their conventional flow tube counterparts. In the post-Laval nozzle flow, there can be no complications due to heterogeneous wall effects.

In the preexpansion region a pulsed cold cathode discharge is used to generate the OH radical or its isotopomer from the radical precursors, H_2O or D_2O, seeded into the N_2 buffer flow. A mixing ratio of 1:100: >1000 of the radical precursor/reactant/N_2 was introduced into the reservoir, thus ensuring pseudo- first-order conditions in the OH/OD radical. The radical concentration was followed by LIF, exciting the $Q_1(1)$ and $Q_{21}(1)$ lines of the (1,0) band of the A $^2\Sigma^+ \leftarrow$ X $^2\Pi$ system for OH near 281.9 nm and for OD near 287.6 nm, while detecting the (1,1) and (0,0) off-resonance fluorescence through a 310 nm notch filter (Corion P310) with a photomultiplier tube perpendicular to the flow. The relative radical concentration, as determined by fluorescence intensity, was measured as a function of flow distance, and therefore reaction time. The excitation is performed in a saturated mode which allows simple confirmation of both OH internal temperature (via scanning excitation wavelengths) and local relative density.

The reported temperatures were measured in the post nozzle flow using LIF, exciting the S_{21} branch of the (1,0) band of the A $^2\Sigma^+ \leftarrow$ X $^2\Pi$ system for OH and detecting the (1,1) and (0,0) off-resonance fluorescence. Rotational line intensities, corrected for line strength factors,[18] are found to be completely described by a Boltzmann distribution and thus yield the local rotational temperature. This rotational temperature allows the derivation of the flow Mach number through the isentropic expansion relationship,[17] as well as provides a direct measurement of the local thermal conditions. These LIF excitation scans were conducted at several flow distances to determine the temperature uniformity of the flow. Flow conditions employed in this work guaranteed flow uniformity better than 10%. Also as a further check of flow uniformity, the velocity of the flow was measured via pitot impact pressure measurements.[17] Temperatures derived from these impact velocities agreed to within 9% of the measured rotational temperatures. In this study all nozzles employed a nitrogen buffer and stagnation or reservior temperatures were held at 300 K. With the Mach number range of these nozzles, a temperature window of 120 to 224 K was accessed.

The absolute HBr and DBr partial pressures prior to delivery to the reservoir were actively monitored through UV absorption measurements at 220 nm, using a 10-cm path flow cell. The absorption cross section for HBr was independently determined using a Beckman DU-40 UV/VIS spectrometer. The absorbances were taken for different pressures of the absorbing gas, HBr or DBr, in a 10.0 cm static cell. These pressures were measured with a capacitance manometer (MKS Baratron 220 CD). The absorption cross section for HBr was found to be σ_{HBr} (220 nm) = 2.49 (±0.10) × 10^{-19} cm^2. This value is in good

TABLE 1: Rate Coefficients for the Reaction of OH + HBr and the Isotopic Variants, with the Experimental Conditions Used for Their Measurements

reaction	temp. (K)	density ($\times 10^{17}$ cm^{-3})	k ($\times 10^{11}$ cm^{3s-1})	ref.
OH + HBr	120	1.65	3.23 (±0.46)	*a*
OH + HBr	141	0.343	2.56 (±0.32)	*a*
OH + HBr	185	1.41	1.72 (±0.40)	*a*
OH + HBr	224	1.04	1.31 (±0.35)	*a*
OH + HBr	230	0.420	1.46 (±0.17)	*b*
OH + HBr	243	0.397	1.20 (±0.14)	*b*
OH + HBr	260	0.371	1.12 (±0.13)	*b*
OH + HBr	278	0.347	1.20 (±0.13)	*b*
OH + HBr	298	0.324	1.11 (±0.12)	*b*
OH + HBr	328	0.294	1.05 (±0.12)	*b*
OH + HBr	360	0.268	0.97 (±0.14)	*b*
OD + HBr	120	1.65	3.45 (±0.59)	*a*
OD + HBr	141	0.343	2.46 (±0.27)	*a*
OD + HBr	185	1.41	1.93 (±0.27)	*a*
OD + HBr	224	1.65	1.45 (±0.22)	*a*
OD + HBr	230	0.420	1.58 (±0.21)	*b*
OD + HBr	243	0.397	1.40 (±0.16)	*b*
OD + HBr	260	0.371	1.21 (±0.11)	*b*
OD + HBr	278	0.347	1.21 (±0.11)	*b*
OD + HBr	297	0.325	1.11 (±0.12)	*b*
OD + HBr	298	0.324	1.22 (±0.14)	*b*
OD + HBr	328	0.294	1.09 (±0.12)	*b*
OD + HBr	360	0.268	1.01 (±0.13)	*b*
OH + DBr	120	1.65	3.22 (±0.30)	*a*
OH + DBr	141	0.343	1.71 (±0.11)	*a*
OH + DBr	185	1.41	0.91 (±0.15)	*a*
OH + DBr	224	1.65	0.65 (±0.14)	*a*
OH + DBr	230	0.420	0.74 (±0.11)	*b*
OH + DBr	260	0.371	0.68 (±0.08)	*b*
OH + DBr	278	0.347	0.64 (±0.08)	*b*
OH + DBr	296	0.326	0.59 (±0.09)	*b*
OH + DBr	328	0.294	0.57 (±0.07)	*b*
OH + DBr	360	0.268	0.60 (±0.11)	*b*
OD + DBr	120	1.65	7.50 (±0.46)	*a*
OD + DBr	141	0.343	3.12 (±0.21)	*a*
OD + DBr	185	1.41	1.36 (±0.13)	*a*
OD + DBr	224	1.65	0.84 (±0.17)	*a*
OD + DBr	230	0.420	0.72 (±0.09)	*b*
OD + DBr	243	0.397	0.74 (±0.11)	*b*
OD + DBr	260	0.371	0.71 (±0.10)	*b*
OD + DBr	278	0.347	0.77 (±0.10)	*b*
OD + DBr	300	0.322	.072 (±0.11)	*b*
OD + DBr	328	0.294	0.66 (±0.09)	*b*
OD + DBr	360	0.268	0.63 (±0.09)	*b*

[a] This work. [b] Bedjanian et al.[15]

agreement with the value measured by Hubert et al.[19] of 2.37 (±0.05) × 10^{-19} cm^2, but falls outside of the value measured by Nee et al.[20] of 3.5 (±0.56) × 10^{-19} cm^2. Further, the absorption cross section for DBr was measured to be σ_{DBr} (220 nm) = 1.24 (±0.05) × 10^{-19} cm^2. To the best of our knowledge, there have been no published measurements of this latter value. As a cross check this setup and procedure was used to measure the absorption cross section for methylbromide at 220 nm, 3.79 (±0.15) × 10^{-19} cm^2. This value is in excellent agreement with previous measured cross sections for CH_3Br.[21,22] This same spectrometer was used for active measurements of flow concentrations. The purity of the gases used were as follows: N_2 > 99.99 (Matheson), HBr > 99.8% (Matheson, degassed of H_2), and DBr > 99% (Cambridge Isotopes, 99% isotopic purity, degassed of D_2).

Results

The results of this investigation are summarized in Table 1, along with a list of the reaction conditions used. Also given are the results of Bedjanian et al., who performed similar temperature-dependent studies of Reactions 1−4 above 230 K using a conventional subsonic flow reactor accompanied by modulated molecular beam mass spectrometric detection.[15] The combined results are presented in Figure 2. Reactions 1−4 have no significant temperature dependence above 200 K, but clearly show inverse temperature dependence at T < 200 K.

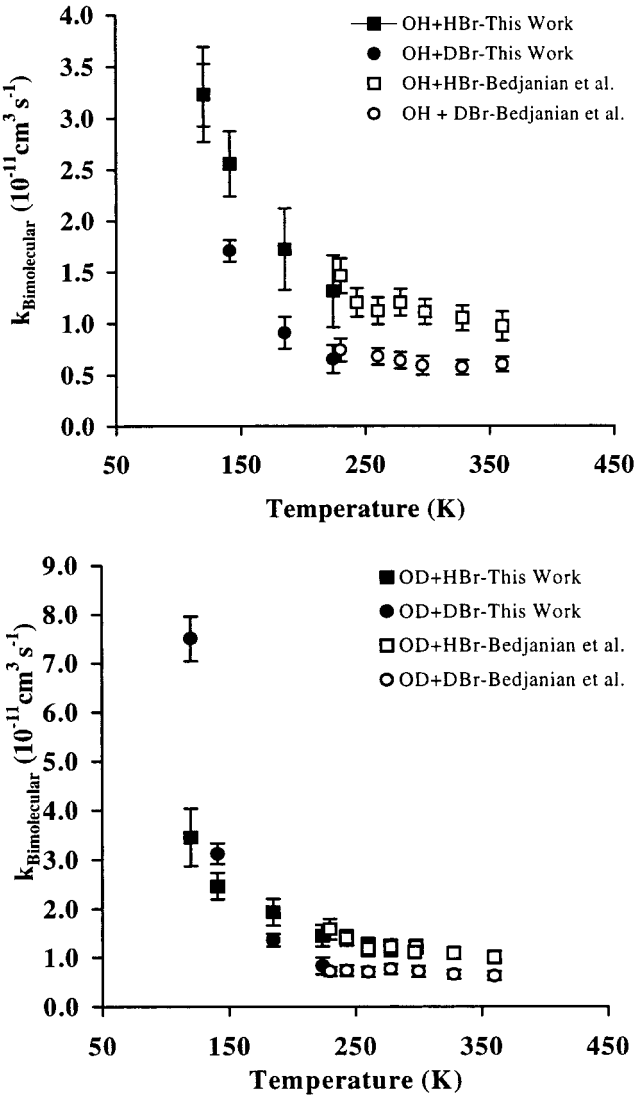

Figure 2. The temperature dependence of the rate coefficients for: OH + HBr; OH + DBr; OD + HBr; OD + DBr are displayed. This work and the results of Bedjanian et al.[15] are included.

The rate coefficients in Table 1 and Figure 2 are all obtained from bimolecular OH/OD loss rate measurements. Two possible reactions can effectively lead to such loss. In the case of OH + DBr, for instance, these are the atom transfer reaction:

$$OH + DBr \rightarrow HOD + Br \quad \Delta H_0^\circ = -126 \text{ kJ/mol} \quad (3)$$

and the isotope exchange reaction:

$$OH + DBr \rightarrow OD + HBr \quad \Delta H_0^\circ = -1.45 \text{ kJ/mol } (E/R = -174 \text{ K}) \quad (5)$$

For the reactant combination OH + DBr, the isotope exchange is exothermic. For all others the isotopic exchange enthalpy is either endothermic, for example in

$$OD + HBr \rightarrow OH + DBr \quad \Delta H_0^\circ = +1.45 \text{ kJ/mol } (E/R = +174 \text{ K}) \quad (6)$$

TABLE 2: Summary of Kinetic Isotope Effects as a Function of Temperature

study	temperature (K)	primary (OH) k_1/k_3	secondary (HBr) k_1/k_2	primary (OD) k_2/k_4	secondary (DBr) k_3/k_4
a	120.0	1.00(±0.17)	0.94(±0.20)	0.46(±0.08)	0.43(±0.05)
a	140.8	1.50(±0.21)	1.04(±0.17)	0.79(±0.10)	0.55(±0.05)
a	185.0	1.90(±0.54)	0.89(±0.24)	1.42(±0.24)	0.67(±0.13)
a	224.0	2.01(±0.68)	0.91(±0.28)	1.73(±0.44)	0.78(±0.23)
b	230.0	1.97(±0.37)	0.92(±0.16)	2.19(±0.40)	1.03 (±0.20)
b	243.0		0.86(±0.14)	1.89 (±0.36)	
b	260.0	1.65(±0.27)	0.93(±0.16)	1.70(±0.32)	0.96(±0.18)
b	278.0	1.88(±0.31)	0.99(±0.16)	1.57(±0.28)	0.83(±0.15)
b	298.0	1.88(±0.35)	0.95(±0.15)	1.62(±0.31)	0.82(±0.18)
b	328.0	1.84(±0.31)	0.96(±0.15)	1.65(±0.29)	0.86(±0.16)
b	360.0	1.62(±0.30)	0.96(±0.19)	1.60(±0.31)	0(.95(±0.18)

[a] This work. [b] Bedjanian et al.[15]

or exchange is of no consequence, (i.e., OD + DBr). However, for both Reactions 5 and 6 we have measured upper limits to the exchange rate coefficients by monitoring OH/OD interchange in the presence of HBr/ DBr. This corresponds, for Reaction 5, to monitoring for exchange product OD when OH is mixed in the presence of DBr. These measurements were carried out at 141 K and no exchange could be detected. For Reaction 5, k_5 (141 K) $< 3 \times 10^{-13}$ cm^3 s^{-1}, and for Reaction 6, k_6 (141 K) $< 5 \times 10^{-13}$ cm^3 s^{-1}. This observation of negligible atom exchange in OH + HBr systems is consistent with the observations of Bedjanian et al. at 298 K.[15] Both of these studies indicate that exchange does not play an important role in OH + HBr kinetics and that direct atom transfer is the dominant mechanism for OH loss. Thus the rate coefficients listed in Table 1 represent those for H/D transfer to the hydroxyl radical to produce bromine atom and water.

To better elucidate the effects of isotopic substitution, the ratios of k_H/k_D were determined for both primary and secondary substitutions. These ratios or kinetic isotope effects are listed in Table 2, and illustrated in Figure 3. The primary KIE for reaction with OD ranges from 2.2 to 0.46, while the primary KIE for reaction with OH varies from 2.0 to 1.0 with decreasing temperature. The secondary KIE values for reaction with DBr range from 1.0 to 0.4, while for reaction with HBr the ratios remain constant near unity. There appears to be a small systematic discrepancy between the highest temperature ratios of this study with the lowest temperature ratios observed by Bedjanian et al. Although the origin of this discrepancy is not entirely clear, we feel the trends observed between both data sets in Figures 2 and 3 suggest a problem in the lowest temperature measurement of Bedjanian et al. In particular, the largest discrepancy occurs regarding the primary kinetic isotope ratio, k_2/k_4. As will be discussed in the next section, there is no fundamental reason a primary kinetic isotope effect should show such a large increase as temperature drops between 260 and 230, whereas we feel that the drop in this ratio below 230 is on sound fundamental foundation. It is important to note however, that all of the data and trends discussed fall within the error limits of both studies and it seems imprudent to apply significance to this minor disagreement.

The observations apparent in the current work from Figure 3 are the first unequivocal experimental documentation of inverse kinetic isotope ratios (the heavier isotopomer having the larger rate coefficient). The 120 K data also show correlation between the pairs k_1/k_3 and k_1/k_2, as well as k_2/k_4 and k_3/k_4. Reactions 2 and 3 form the same products, HOD and Br. Thus, the ratio pairs, k_1/k_3 and k_1/k_2, would seem to compare reactions producing H_2O product to those producing HOD while the pairs, k_2/k_4 and k_3/k_4, compare reactions producing HOD against one

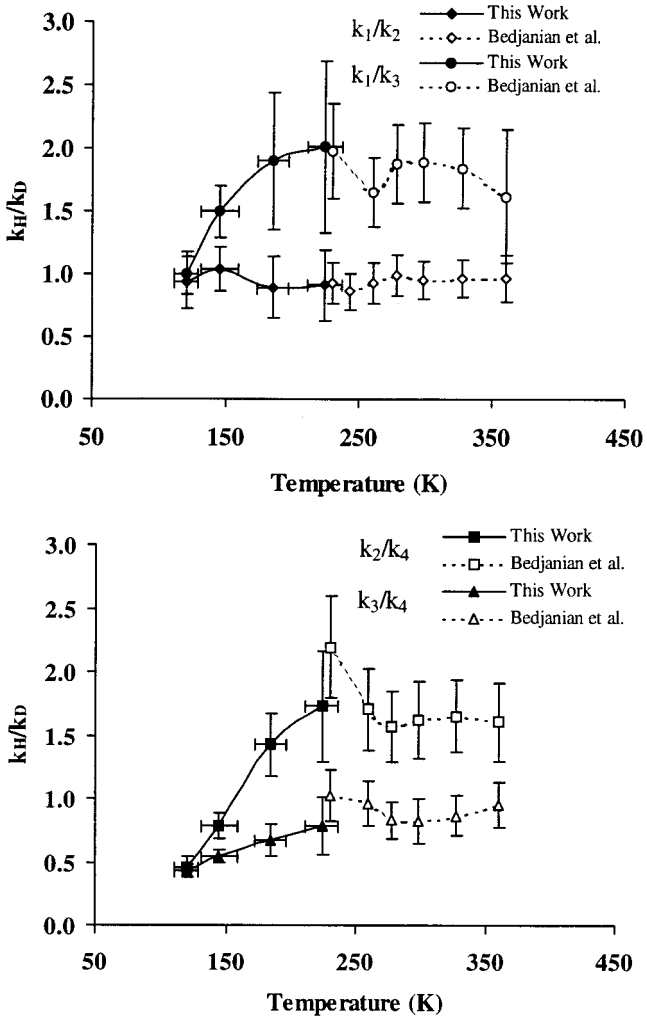

Figure 3. The ratios of the measured rate coefficients, for primary (k_1/k_3 and k_2/k_4) and secondary (k_1/k_2 and k_3/k_4) kinetic isotope effects, plotted versus temperature. This work and the results of Bedjanian et al.[15] are included.

generating D_2O product. It thus appears that while high-temperature kinetic isotope ratios in these reactions tend to correlate to reactant states (thus, the individuality of primary and secondary effects), the correlation at low temperatures seems to be with product channels. At 120 K, it appears that the concept of primary and secondary KIE has vanished for this reaction.

Discussion

Reactions with inverse temperature dependent rate coefficients are well-known in collision systems with strong long-range attractive forces. Such behavior in radical−molecule systems has long been fit using Arrhenius rate laws and since the activation energy, E_a, is typically defined as −R times the slope of a plot of ln k vs 1/*T*, these reactions have been termed as possessing negative activation energies. Using statistical arguments, Mozurkewich and Benson have demonstrated how reactions on long range attractive surfaces can manifest negative activation energies if they possess a late tight transition state which follows a loose one early in the entrance channel.[23] Such a system leads naturally to a long-lived collision complex and the branching of this complex between products (through the tight transition state) and reactants (through the loose entrance channel barrier) naturally leads to inverse temperature dependence in the reactive rate coefficient. This model is only

appropriate to reaction systems in a temperature regime where the reaction efficiency is much less than unity. In the temperature range between 120 and 300 K, Reaction 1 is calculated to have a dipole−dipole capture collision rate coefficient approximately 10 to 20 times greater than the observed reaction rate coefficient and so such a model may be appropriate.[24] While the complex model places emphasis on entrance channel effects governing the overall temperature dependence of the rate coefficient, kinetic isotope ratios would be sensitive to the state density in the tight transition state. The model predicts in such circumstances that deuteration of reactants can lead to inverse primary kinetic isotope effects since the state density in the deuterated transition state is increased and the zero point energy lowered, which lowers the effective activation energy and increases the rate of passage to products. This prediction is supported by similar modeling of McEwen and Golden.[25] To date, these predictions have not been supported by experimental observation of inverse KIEs, though several studies have reported normal primary kinetic isotope ratios which display weak inverse temperature dependence.

Battin-Leclerc et al. studied the temperature dependence (T = 200 to 400 K) of kinetic isotope effects in the reaction of OH + HCl and all H/D isotopic variants.[26] They observed that the primary kinetic isotope effect increases as temperature decreases which is contrary to what is observed in the present study of OH + HBr. However, this reaction is known to have a positive activation barrier at these temperatures. Their observation of an inverse secondary kinetic isotope effect is in accord with what is observed in this study and has been argued as a natural consequence of secondary effects of deuteration on the zero point energy of the transition state. In fact, effective barrier calculations suggested the largest positive barrier exists for the OH + HCl reaction with barriers decreasing monotonically across the series OH + DCl, OD + HCl, and OD + DCl. From this result, it is not immediately clear why an inverse primary KIE was not observed in that study.

The reaction of H + HBr and its isotopic variants have also been studied from 214 to 300 K.[27] Unlike the present system of OH + HBr, this reaction has a large positive temperature dependence (E_a/R = 400 K − 790 K) and apparently adheres well to an Arrhenius rate form with a positive activation energy. The measured isotope effects were normal, increasing with lower temperature unlike the behavior observed for the present system. Nicovich et al. have studied primary kinetic isotope effects of alkyl radicals with HBr/DBr.[28] These systems were found to have negative activation energies, thus increasing rates as temperature is decreased, similar to the present system. They also found that as the activation energy becomes more negative, the magnitude of the primary kinetic isotope effect is reduced. It should be noted that these studies were done at temperatures greater than 250 K. Unfortunately this work has not been extended to temperatures beyond those for which the KIE is anything but normal.

The observed temperature dependence of Reaction 1 is well fit by a T^{-n} functional dependence where n is approximately 0.9, but does not fit well to a strict Arrhenius rate law with a temperature-independent activation energy.[13−16] This inverse temperature dependence is consistent with the best available potential surface (LEPS) which displays no barrier for this exoergic reaction. Quantum scattering calculations on the ground electronic LEPS surface (Clary potential) predicts a $T^{-1/2}$ dependence in the rate coefficient which when convolved with the electronic partition coefficient between the OH $^2\Pi_{1/2}$ excited and $^2\Pi_{3/2}$ ground states accurately predicts the observed behavior of $k_1(T)$.[29] Unfortunately, parametrization of these results as a function of OH and HBr rotor constant suggest kinetic isotope ratios, k_H/k_D, of $2^{1/2}$ independent of OH or HBr substitution site. More recent quasi-classical trajectory calculations on this same qualitative (Clary) PES and another (Modified potential) adjusted to fit better the observed H_2O product state vibrational energy distributions have been performed at 300 K for Reactions 1 and 2.[30] These results slightly over-predict the experimentally observed 300 K rate coefficients and, contrary to observation, predict an inverse secondary kinetic isotope ratio k_1/k_2(300 K) of 0.76.

Nizamov et al. have performed variational transition state theory (VTST) on both the Clary and Modified potentials identifying a transition state lying early in the entrance channel to this reaction.[30] The OH and H′Br bond distances are approximately 0.974 and 1.42 Å, respectively, while the critical O′H distance is between 1.95 and 2.15 Å. The potential energy barrier for these transition states is between −7.20 and −7.45 kJ mol^{-1}; however, the harmonic zero point energy (ZPE) corrected value is very close to 0 (−0.5 kJ mol^{-1} for the Clary potential and +0.25 kJ mol^{-1} for the Modified potential). As expected for such an attractive surface, the harmonic ZPE corrected barrier for Reaction 2, even on the modified surface is lower (−0.96 kJ mol^{-1}). From these results, it is not surprising that even at 300 K, VTST on these surfaces predicts strong inverse primary and secondary kinetic isotope ratios at 300 K with k_1/k_3(300 K) between 0.85 and 0.76, while for k_1/k_2(300 K) they obtain values between 0.8 and 0.72 depending on the potential used. The inverse secondary isotope effect is attributed to the differences of the HOD and HOH′ bend frequencies, and the inverse primary kinetic isotope effect is thought to be a result of the smaller zero point adjusted barrier due to the isotopic substitution. Again, as seen in Table 2 and Figure 3, these experimental 300 K kinetic isotope ratios are found to be essentially k_1/k_3(300 K) = 1.8 for primary substitution and k_1/k_2(300 K) = 1 for secondary substitution within the errors. Though the trends of the VTST secondary KIE results agree with the current low-temperature observations, the absolute values calculated for the secondary KIEs do not agree with experimental results even below 300 K. Nizamov et al. suggest that VTST has difficulty predicting accurate isotope effects when the transition state is early in nature as was employed for this system. However, it needs to also be realized that the potentials employed for all of these models are semiempirical.

It appears that although inverse kinetic isotope effects have been predicted for reactions on purely attractive surfaces, for the OH + HBr reaction in particular, current level of knowledge governing the OH + HBr potential or the ability to model the dynamics in accurate trajectory calculations prohibits a global description of the reaction mechanism. Scattering approaches which incompletely model reactant rotation, and thereby dipole−dipole coupling, appear to be reasonably successful in describing the gross features of the temperature dependence of the rate coefficient (but still not an accurate absolute value), as well as product state energy disposal. Aspects of statistical rate theory and variational transition state theory appear to successfully predict manifestation of inverse kinetic isotope effects but quantitatively fail to predict sensitive dependence on temperature. The very fine balance between positive and negative ZPE corrected activation energies between isotopomeric reactions may play a role here. The effect of H_2O, HOD, and D_2O vibrational frequencies in governing the sign of E_a may place this reaction in a situation where the effective activation energy

(a temperature-dependent function in cases of negative E_a) is only significantly negative at reactant energies below 200 K. In this low-temperature limit, both $k(T)$ and the KIE ratios would be expected to display inverse behavior as is observed. In the high-temperature limit, where the transition state has population in modes above the ZPE level the system may manifest positive or zero E_a values with normal KIE ratios. Unfortunately, the observed $k(T)$ behavior above 250 K for Reactions 1−4 does not suggest the presence of a sufficiently positive activation energy to support the large primary KIE values seen at the higher temperatures.

In heavy−light−heavy reaction systems such as this where both reactants are hydrides and the vibrational frequencies are generally high, the low-temperature limit, as nearly reached at 120 K in this study, leads to reaction on extremely few rovibronic surfaces. In the case of activation energies nearly zero in value, and with a potential surface governed strongly by dipole−dipole forces, molecular rotation in the reactants and thus bending modes in the transition state are expected to play a key role in the low energy reaction dynamics and energetics. It would appear from all of the models that the qualitative picture of the low-temperature behavior of this reaction is well explained, owing to effects of deuteration on transition state zero point energy for strongly attractive reaction potentials. Quantitative agreement between models and the low-temperature results, as well as explanation of the precise dynamics leading to such a rapid transition to normal KIE values and flat $k(T)$ dependence at only modestly higher temperatures, is now clearly needed. Certainly determination of a precise reaction PES would assist this, as may refinement of the treatment of rotations in the scattering models. On the experimental side, extension of the current results below 120 K would be useful to determine the 0 K limit of the KIE values, as well as measurements of the low-temperature rates and KIE values for other comparable systems such as OH + HI, CN + HI, and alkyl radical + hydrogen halides. Any of these results would be expected to add critical insight into the detailed nature of energy dependent dynamics on attractive reaction potentials.

Conclusion

The present study provides new low-temperature kinetic data (120−224 K) for the OH + HBr system and all of the H/D isotopic variants. Below 200 K there is strong temperature dependence in the kinetic isotope effects. This study provides the first experimental observation of inverse primary kinetic isotope effects in a hydrogen transfer reaction. These results provide a foundation for comparison with accurate theoretical treatments on high quality potential surfaces, which are now clearly needed before detailed understanding of this complex chemical reaction will be possible.

Acknowledgment is made to the National Science Foundation and to the donors of the Petroleum Research Fund, administered by the American Chemical Society, for the partial support of this research.

References and Notes

(1) Storzer, H.; Zielinsky, M.; Stutzki, J.; Sternberg, A. *Astron. Astrophys.* **2000**, *358* (2), 682.

(2) Lopate, C. *J. Geophys. Res.* **2000**, *105* (A9), 21005.

(3) Aikawa, Y.; Herbst, E. *Astrophys. J.* **1999**, *526*, 314.

(4) Krankowsky, D.; Mauersberger, K. *Science* **1996**, *274* (5291), 1324.

(5) Chipperfield, M. P.; Shallcross, D. E.; Lary, D. J. *Geophys. Res. Lett.* **1997**, *24* (23), 3025.

(6) Husain, D.; Plane, J. M. C. *J. Chem. Soc., Faraday Trans. 2* **1981**, *77*, 1949.

(7) Takacs, G. A.; Glass, G. P. *J. Phys. Chem.* **1973**, *77* (8), 1060.

(8) Smith, I. W. M.; Zellner, R. *J. Chem. Soc., Faraday Trans. 2* **1974**, *70*, 1045

(9) Ravishankara, A. R.; Wine, P. H.; Langford, A. O. *Chem. Phys. Lett.* **1979**, *63* (3), 479.

(10) Jourdain, J. L.; Le Bras, G.; Combourieu, J. *Chem. Phys. Lett.* **1981**, *78* (3), 483.

(11) Cannon, B. D.; Robertshaw, J. S.; Smith, I. W. M.; Williams, M. D. *Chem. Phys. Lett.* **1984,** *105* (4), 380.

(12) Ravishankara, A. R.; Wine, P. H.; Wells, J. R. *J. Chem. Phys.* **1985**, *83* (1), 447.

(13) Sims, I. R.; Smith, I. W. M.; Clary, D. C.; Bocherel, P.; Rowe, B. R. *J. Chem. Phys.* **1994**, *101* (2), 1748.

(14) Atkinson, D. B.; Jaramillo, V. I.; Smith, M. A. *J. Phys. Chem. A* **1997**, *101*, 3356.

(15) Bedjanian, J.; Riffault, V.; Le Bras, G.; Poulet, G. *J. Photochem. Photobio. A: Chem.* **1999**, *128*, 15.

(16) Jaramillo, V. I.; Gougeon, S.; Le Picard, S. D.; Canosa, A.; Smith, M. A.; Rowe, B. R. *Int. J. Chem. Kinet.*, accepted for publication.

(17) Atkinson, D. B.; Smith, M. A. *Rev. Sci. Instrum.* **1995**, *66*, 4434.

(18) Luque, J.; Crosley, D. R. "LIFBASE: Database and Spectral Simulation Program (Version 1.2)"; SRI International Report MP 98-021, 1998.

(19) Huebert, B. J.; Martin, R. M. *J. Phys. Chem.* **1968**, *72* (8), 3046.

(20) Nee, J. B.; Suto, M.; Lee, L. C. *J. Chem. Phys.* **1986**, *85* (9), 4919.

(21) Robbins, D. E. *Geophys. Res. Lett.* **1976**, *3* (4), 213.

(22) Molina, L. T.; Molina, M. J.; Rowland, F. S. *J. Phys. Chem.* **1982**, *86*, 2672.

(23) Mozurkewich, M.; Benson, S. W. *J. Phys. Chem.* **1984**, *88*, 6429.

(24) Clary, D. C.; Stoecklin, T. S.; Wickham, A. G. *J. Chem. Soc., Faraday Trans.* **1993**, *89*, 2185.

(25) McEwen, A. B.; Golden, D. M. *J. Mol. Struct.* **1990**, *224*, 357.

(26) Battin-Leclerc, F.; Kim, I. K.; Talukdar, R. K.; Portmann, R. W.; Ravishankara, A. R.; Steckler, R.; Brown, D. *J. Phys. Chem. A* **1999**, *103*, 3237.

(27) Umemoto, H.; Wada, Y.; Tsunashima, S.; Takayanagi, T.; Sato, S. *Chem. Phys.* **1990**, *143*, 333.

(28) Nicovich, J. M.; van Dijk, C. A.; Kreutter, K. D.; Wine, P. H. *J. Phys. Chem.* **1991**, *95*, 9890.

(29) Clary, D. C.; Nyman, G.; Hernandez, R. *J. Chem. Phys* **1994**, *101* (5), 3704.

(30) Nizamov, B.; Setser, D. W.; Wang, H.; Peslherbe, G. H.; Hase, W. L. *J. Chem. Phys.* **1996**, *105* (22), 9897.